

Alkylammonium-Based Protic Ionic Liquids. II. Ionic Transport and Heat-Transfer Properties: Fragility and Ionicity Rule

Mérièm Anouti,* Magaly Caillon-Caravanier, Corinne Le Floch, and Daniel Lemordant

Laboratoire CIME (EA2098), Université François Rabelais, Parc de Grandmont 37200, Tours, France

Received: April 22, 2008; Revised Manuscript Received: May 16, 2008

The physicochemical characterization of six alkylammonium-based protic ionic liquids (PILs) is presented. These compounds were prepared through a simple and atom-economic neutralization reaction between a tertiary amine and a Brønsted acid, HX, where X^- is $HCOO^-$, CH_3COO^- , HF_2^- . The temperature dependency and the effect of added water on properties such as density, viscosity, ionic conductivity, and the thermal comportment of these PILs were measured and investigated. The results allowed us to classify them according to a classical Walden diagram and to appreciate their great “fragility”. PILs have applicable perspectives in replacements of conventional inorganic acids for fuel cell devices and thermal transfer fluids.

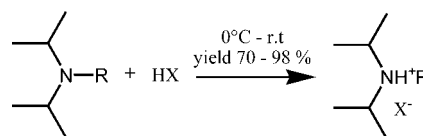
1. Introduction

An ionic liquid (IL) is usually defined as a substance comprised of ions, typically with one ion being an organic species, with a melting temperature of less than 100 °C. ILs have been developed and studied extensively during the last 10 years.^{1,2} Room-temperature ionic liquids (RTILs) are a “sub-category” of ILs which are liquid at temperatures less than 25 °C.³ The first IL extensively studied was 1-ethyl-3-methylimidazolium chloroaluminate ($EMImAlCl_4$).⁴ However, chloroaluminate ionic liquids are hydrolyzed by traces of water, which limits their use. More recently, ILs consisting of large organic, asymmetrical ions, such as 1,3-dialkylimidazolium, 1-alkylpyridinium, 1-alkylpyrazolium, tetraalkylammonium, or tetraalkylphosphonium cations and BF_4^- , PF_6^- , $CF_3SO_3^-$, or $N(SO_2CF_3)_2^-$ anions have been developed.^{1,5} The intrinsic properties of ILs can be varied by simply combining different cations or anions. Thus, specific demands for a synthesis or chemical process can be met by optimally tailoring the ionic liquid. The most advantages attributed to ILs are (i) a thermal stability which allows the use of these solvents in a larger temperature range than conventional solvents; a wide range liquid phase (up to 300 or 400 °C in some cases) is able to facilitate processes; (ii) a high electrochemical stability and a large electrochemical window opens the whole range of electrochemical applications; (iii) low vapor pressure reduces the loss of liquid into the environment (“green chemistry”); (iv) adjustable solubility permits us to design hydrophobic as well hydrophilic ionic liquids.

Among the most important properties in terms of potential application as electrolytes in electrochemical devices is their conductivity. A great number of studies concern ILs’ specific conductivity, in their pure liquid state as well as solutions in molecular solvents or in a mix with polymers.^{6–10} Typical ionic liquids have aprotic structures and do not have chemically active protons,^{11–15} but proton-transfer salts obtained from Brønsted acid/base pairs are additional candidates for the preparation of protic ionic liquids (PILs) and proton conductors.^{16–20}

This work is a continuation of a previous study,²¹ which is devoted to the preparation and physicochemical characterizations of alkylammonium-based PILs prepared through a simple and atom-economic neutralization reaction between a tertiary amine

SCHEME 1: Preparation of PILs



and a Brønsted acid, HX, where X^- is $HCOO^-$, CH_3COO^- , HF_2^- . The temperature dependency and the effect of added water on some properties such as density, viscosity, ionic conductivity, and the thermal comportment of these PILs have been measured and investigated in detail. The results allowed us to classify them according to a classical Walden diagram and to appreciate their great “fragility”. PILs have applicable perspectives in replacements of conventional inorganic acids for fuel cell devices and thermal transfer fluids.

2. Experimental Section

2.1. Materials. The bases *N*-diisopropylethylamine DIEA (99+%) and *N*-diisopropylmethylamine DIMA (99+%) were obtained from Aldrich Chemical Co. Anhydrous acetic acid (HAc, 99+%), anhydrous formic acid (HFm, 98%), and hydrofluoric acid 50% in water were obtained from Fluka. All chemicals were used as received. Water is purified with a Milli-Q 18.3 MΩU water system.

2.2. General Procedures for the Preparation of *N*-Alkylamine-Based PILs. All ionic liquids used in this study are synthesized according to the procedure described in part 1 of this article,²¹ by neutralization of tertiary amines with suitable acids. The preparation is easy by just mixing these two components equimolarly which gave salts composed of protonated ammonium cations and corresponding acid anions (see Scheme 1). The preparation of *N*-alkylamine-based PILs and the abbreviations used to design them are indicated, respectively, in Scheme 1 and Table 1.

3. Measurements

Density values were determined by measuring the weight of samples filling a 5 mL picnometer volumetric flask at 25 °C. Before each measurement, the flasks were maintained at 25 °C in a thermostatted JULABO circulating water bath for half an hour until the temperature was steady. A series of measurements with distilled water is used to calibrate the picnometer. The accuracy is better than 0.5%. Viscosities of pure PILs and their

* Corresponding author. E-mail: meriem.anouti@univ-tours.fr. Fax: (33)247367360. Tel.: (33)247366951.

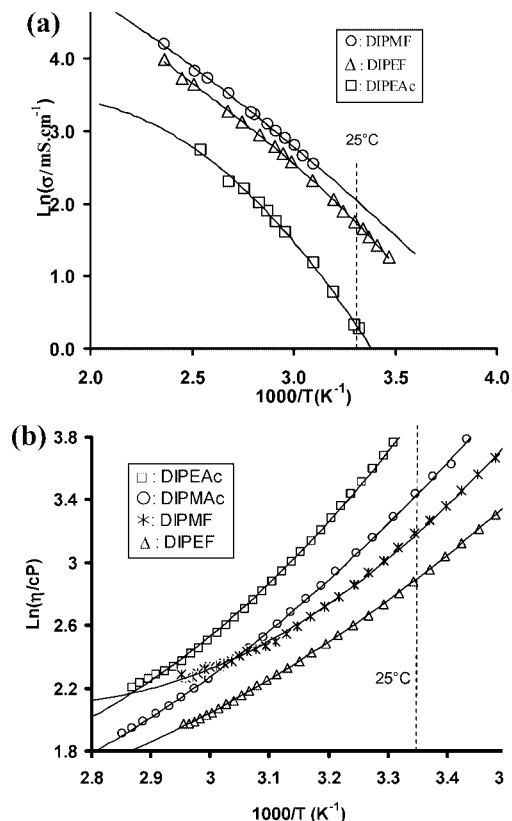
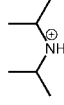
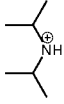


Figure 1. Arrhenius plot for the ionic conductivities (a) and viscosities (b) for some ionic liquids presented in this work.

TABLE 1: PIL Names and Abbreviations Used in This Work

Cation	Anion	Name	Abbreviation
	HCOO ⁻	Diisopropylethylammonium formate	DIPEF (1a)
	CH ₃ COO ⁻	Diisopropylethylammonium acetate	DIPEAc (1b)
	HF ₂ ⁻	Diisopropylethylammonium hydrogenobisfluoride	DIPEHF (1c)
	HCOO ⁻	Diisopropylmethylammonium formate	DIPMF (2a)
	CH ₃ COO ⁻	Diisopropylmethylammonium acetate	DIPMAc (2b)
	HF ₂ ⁻	Diisopropylmethylammonium hydrogenobisfluoride	DIPMHF (2c)

mixture with water are measured using a TA instrument rheometer (AR 1000) with conical geometry at temperatures ranging from 25 to 80 °C. Ionic conductivities are measured using a Crison (GLP 31) digital conductimeter at several frequencies. The temperature control (from 20 to 200 °C) is

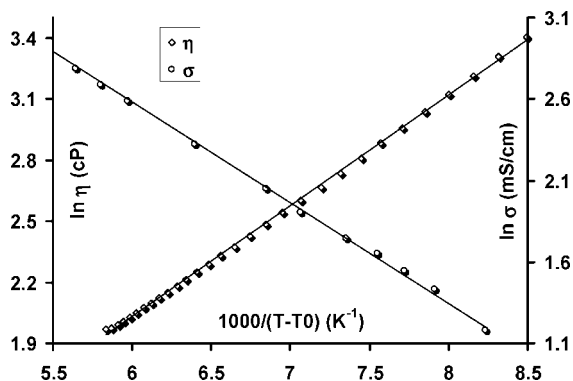


Figure 2. VTF plot of ionic conductivities and viscosities for DIPEF.

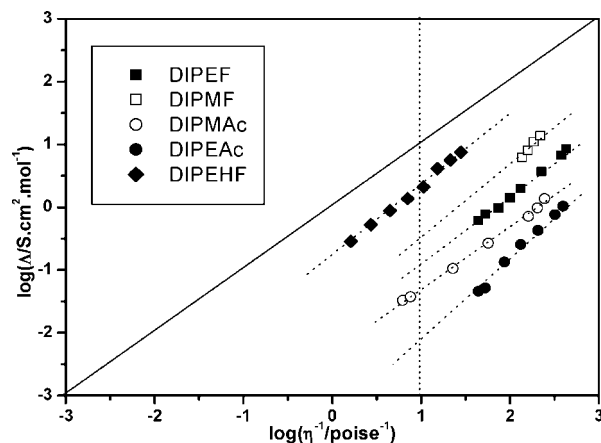


Figure 3. Walden plots for protic ionic liquids (PILs).

ensured by a JULABO thermostatted oil bath. Differential scanning calorimetry (DSC) is carried out on a Perkin-Elmer DSC6 under a N₂ atmosphere. Samples for DSC measurements are sealed in Al pans. Thermograms are recorded during heating (from 10 to 400 °C) with a scan rate of 10 °C·min⁻¹.

All PILs–water mixtures were prepared by mass using a balance with a sensitivity of 0.1 mg. Mixtures were prepared by diluting the pure PILs by a known amount of Milli-Q water in order to obtain the required concentration.

3.1. Effect of Temperature on Conductivities and Viscosities of PILs. The ionic conductivities of the six ionic liquids studied are determined in the range of 20–120 °C. The results, which are summarized in Table 2, show that PILs possess good ionic conductivity at 25 °C (1.3 mS·cm⁻¹ (1b) < σ < 8.2 mS·cm⁻¹ (2a)) and higher better values are obtained at 100 °C (10.0 mS·cm⁻¹ (1b) < σ < 42.9 mS·cm⁻¹ (2c)). The best conductivities are obtained when at the same time the cation and the anion are of small size (2c).

This evolution of conductivity can be attributed to several factors, such as the geometrical and electronic structure of the cation and anion, hydrogen-bond interactions, diffusion coefficient of the proton, and lower viscosity of the PILs [18 cP (1a) < η < 100 cP (2c) at 25 °C, see Figure 1b].

The temperature dependency of the ionic conductivity and viscosity for DIPEF, DIPMF, DIPMAc, and DIPEAc are studied, and their Arrhenius plots are depicted in Figure 1, parts a and b. The relationship of temperature dependency of the ionic conductivity and viscosity shows an apparent convex-curved profile.

The temperature dependency of the ionic conductivity and viscosity can be fitted to the Vogel–Tamman–Fulcher (VTF) equation:

$$\sigma = \sigma_0 \exp\left[\frac{-B}{(T - T_0)}\right] \quad (1)$$

$$\eta = \eta_0 \exp\left[\frac{B'}{(T - T_0)}\right] \quad (2)$$

where σ₀ (mS·cm⁻¹), B (K), η₀ (cP), B' (K), and T₀ (K) are fitting parameters. As an example, in Figure 2 are plotted ln(σ) and ln(η) versus 1000/(T - T₀) based on the VTF eqs 1 and 2 for DIPEF. The product BR (R is the molar gas constant) is equivalent to an activate energy (kJ·mol⁻¹) which is not calculated in this paper. The best-fit σ₀ (mS·cm⁻¹), B (K), and T₀ (K) parameters are given in Table 3.

One way of assessing the ionicity of ionic liquids is to use the classification diagram based on the classical Walden rule.²²

TABLE 2: Ionic Conductivities in $\text{mS}\cdot\text{cm}^{-1}$ for PILs at 25 and 100 °C

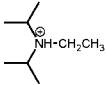
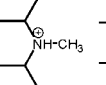
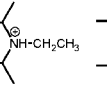
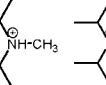
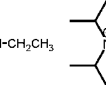
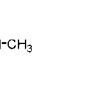
	1a	2a	1b	2b	1c	2c
anion	HCOO^-	HCOO^-	CH_3COO^-	CH_3COO^-	HF_2^-	HF_2^-
cation						
25°C	5.0	8.2	1.3	1.6	3.4	7.6
100°C	26.6	33.5	10.0	10.4	28.5	42.9

TABLE 3: VTF Equation Parameters for Ion Conductivity (σ_0 , B , T_0) and Viscosity (η_0 , B' , T_0) (Eqs 1 and 2 in the Text)

ionic liquids	T_g (K) ^a	T_0 (K)	σ_0 ($\text{mS}\cdot\text{cm}^{-1}$)	B (K) ^c	R^2 ^b	η_0 (cP)	B' (K) ^c	R^2 ^b
DIPEF (1a)	170	167	538.4	617.9	0.9994	0.29	544.2	0.9995
DIPMF (2a)	169	167	684.1	622.3	0.9995	0.20	632.0	0.9994
DIPEAc (1b)	182	179	417.3	703.5	0.9995	0.08	771.5	0.9996
DIPMAc (2b)	172	170	402.8	699.5	0.9991	0.135	699	0.9993
DIPEBF (1c)	218	204	388.3	444.6	0.9996	0.8266	430.2	0.9996
DIPMBF (2c)	200	198	412.9	400	0.9994	n.d.	n.d.	n.d.

^a Refer to part 1 of this article (ref 21). ^b Correlated coefficient. ^c $BR \equiv$ activate energy ($\text{kJ}\cdot\text{mol}^{-1}$).

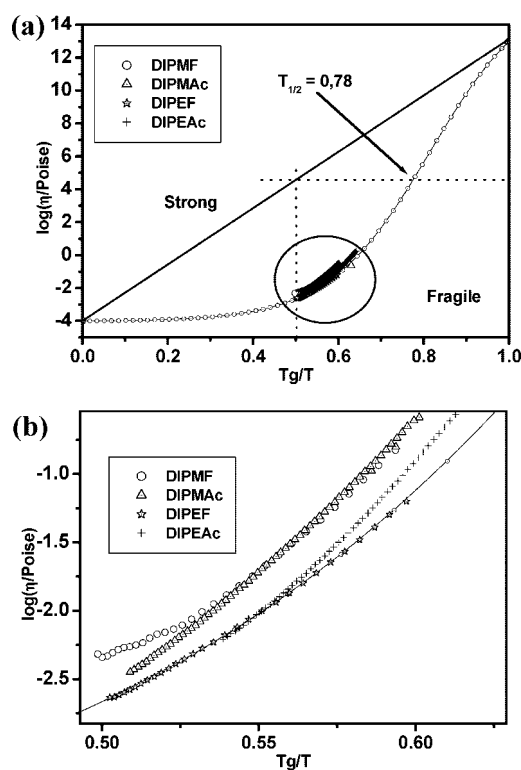


Figure 4. Fragility plot for a selection of four PILs of this study (a); zoom in the circle (b).

The Walden rule relates the ionic mobilities represented by the equivalent conductivity Λ to the fluidity η^{-1} of the medium through which the ions move. The ideal line (see Figure 3) is obtained on the basis that ions have mobilities that are determined only by the viscosity of the medium and that the number of ions present in the equivalent volume is that indicated by salt composition (i.e., all ions contribute equally);^{22,23} the position of the ideal line is established using aqueous KCl solutions at high dilution.

With specific conductivity σ data of Figure 1, the equivalent conductivities Λ are calculated by use of the relation $\Lambda = V_e \sigma$ where V_e is the equivalent volume. The results obtained for five PILs are plotted in Figure 3.

TABLE 4: Glass Transition Temperature (T_g) and Fragility Parameters for PILs

substance	T_g (K)	$T_g/T_{1/2}$	$F_{\text{kin},1/2}$
DIPEF	170	0.78	0.56
DIPMF	169	0.78	0.56
DIPEAc	182	0.78	0.56
DIPMAc	172	0.78	0.56
DIPEHF	218	0.76	0.52
DIPEBF	200	n.d.	n.d.
0.6KNO ₃ , 0.4Ca(NO ₃) ₂ (fragile) ^a	340	0.82	0.64
GeO ₂ (strong) ^a	810	0.55	0.24

^a Ref 37.

All PILs studied in this work are conforming to the Walden rule. Indeed, they lie significantly closer to the ideal line with unit slope than aprotic ILs like quaternary ammonium tetrafluoroborate.^{14,24,25} Figure 3 also shows that *N*-diisopropylethylammonium hydrogen bisfluoride is the one that conforms most closely to the Walden rule with $\Lambda\eta$.

The bisfluoride anion HF_2^- has been recently considered as a component of PILs^{26,27} as it is stable in ordinary conditions. Its stability is due to the existence of a strong hydrogen bond between the anion and the additional acid molecule. These ions (HF_2^-) confer to the ionic liquids, when they are associated with a same cation, a better ionic mobility and a greater fluidity compared to formate (HCOO^-) and acetate (CH_3COO^-) ions. This is probably due to their size and their density of charge. Such anions (HF_2^-) could serve as the proton-transporting media in high-temperature fuel cells.

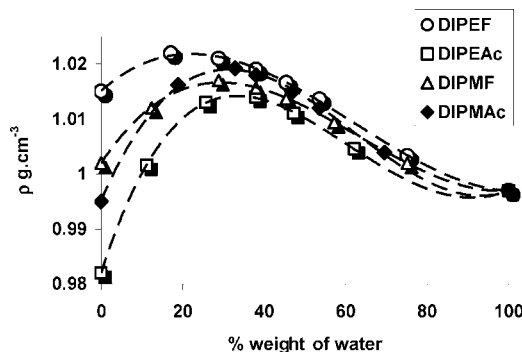
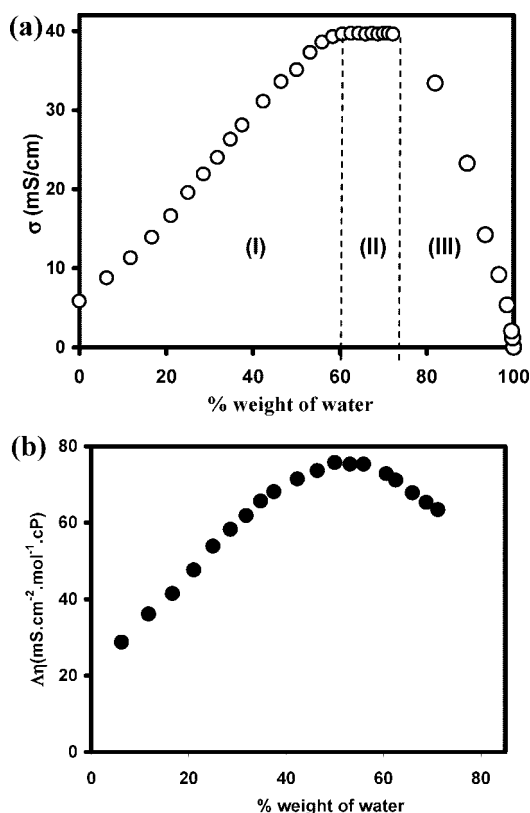
3.2. Fragility of Protic Ionic Liquids Studied. Fragility is a novel concept applicable to the study of the behavior of glass-forming liquids. In a simplified picture, fragility is associated with the profile of the potential energy surface, and it increases with the mean amplitude and variance of the activation barriers. Moreover, this parameter is due to minima in the energy landscape (i.e., the number of accessible molecular configurations). Several approaches have been made to quantify fragility in glassy state physics.^{28,29} Fragility itself has been quantified in various ways.

(i) Very early, Angell et al.³⁰ defined fragility (F) as $F = 1/D$ where D is an exponent parameter in the VTF equation written as $\eta = \eta_0 \exp[(DT_0)/(T - T_0)]$.

(ii) Donth³¹ and Hodge³² related fragility (F) to the ratio $F = T_0/T_g$ when T_0 and T_g are, respectively, the “ideal” glass

TABLE 5: Heat Capacity (C_p) and Heat Storage Density (D_h) for PILs^a

PILs	DIPEF	DIPMF	DIPEAc	DIPMAc	DIPEHF	DIPMHF	BMIImBF ₄ ^b
C_p at 298 K ($J \cdot g^{-1} \cdot K^{-1}$)	2.66	2.69	2.21	2.18	2.47	2.19	1.63
D_h ($\Delta T = 100$ °C) ($MJ \cdot m^{-3}$)	270	264	217	217	248	231	195

^a $D_h = \rho C_p \Delta T$. ^b Ref 38.**Figure 5.** Specific gravity vs weight percentage of water in PIL–water mixtures for some PILs. The dashed lines represent the best fit of the data obtained by regression analysis.**Figure 6.** Variation of ionic conductivity (a) and Walden factor $\Delta\eta$ (b) vs the weight percentage of water in the aqueous DIPEF solution at 25 °C.

transition temperature (T_0) and glass transition temperature (T_g). This ratio conveniently lies between 0 (strong) and 1 (fragile).

(iii) Böhmer and Angell³³ established a relation between the “fragility index” m and the characteristic temperatures T_g and T_0 : $m/(m - 17) = T_g/T_0$; 17 is the lower fragility limit.³⁴

(iv) More recently, Richert and Angell³⁵ also related fragility to relaxation times in an indirect manner. Accordingly, a more convenient $F_{1/2}$ (not F) fragility is given by $F_{kin,1/2} = 2(T_g/T_{1/2}) - 1$, where $T_{1/2}$ is the temperature at which $\log \eta$ is halfway the above range (see Figure 4a). It is this last relation which we have adopted for fragility determination.

TABLE 6: Polynomial Coefficients of the Best Fit of Specific Gravity, ρ ($g \cdot cm^{-3}$), versus Weight Percentage of Water to the Polynomial Expression Given by Eq 3 for PILs

ILs	$A_3 (\times 10^{-7})$	$A_2 (\times 10^{-5})$	$A_1 (\times 10^{-4})$	A_0	R^2
DIPEF	0.986	−1.828	6.613	1.015	0.9990
DIPEAc	2.374	−4.391	2.166	0.982	0.9991
DIPMF	1.273	−2.421	1.099	1.002	0.9993
DIPMAc	1.968	−3.668	1.719	0.995	0.9993

A plot of $\ln(\eta)$ versus the scaled temperature T_g/T is more useful in visualizing comparative fragilities. Angell³⁶ has classified glass-forming liquids as “strong” and “fragile” on the basis of such a plot. Arrhenius liquids are described as strong, whereas those following the VTF equation are fragile. In contrast to strong liquids, viscosities of fragile liquids exhibit a pronounced divergence near T_g .

In Figure 4, we plot the data for a selection of four PILs. The fragility index parameters $F_{kin,1/2}$ (relation in (iv)) are collected in Table 4. It can be seen that the PILs are very fragile compared to extremely “fragile” minimal salts like the mixture (0.6KNO₃, 0.4Ca(NO₃)₂).³⁷ Moreover, the agreement of the T_0 temperatures and T_g (see Table 3) in the VTF treatment confirms that the studied PILs are very fragile.

Protonic ILs which have large hydrogen-bonding contributions to interparticle interactions will therefore tend to have the most extended intermediate range order.

3.3. Heat Capacity and Sensible Heat Storage Density.

The capacity of ionic liquids for storing heat is a crucial quantity for several industrial applications, like solar energy collection and storage at high temperature and refrigeration systems. Sensible heat storage is easily calculated from heat capacity (C_p), density, and the temperature change chosen ($D_h = \rho C_p \Delta T$). In order to calculate the sensible heat storage density of the ILs, heat capacity is determined at 25 °C. The heat capacities (C_p) and heat storage densities (D_h) for DIPEF, DIPEAc, DIPMF, DIPMAc, DIPEHF, DIPMHF, and aprotic ILs BMIImBF₄³⁸ (for comparison) are summarized in Table 5.

It can be seen that the heat capacities of the alkylammonium-based ILs are higher than that of BMIImBF₄ and anions have a more apparent effect on heat capacity than cations. D_h ($MJ \cdot m^{-3}$) = 270–264 for HCOO[−], 248–231 for HF₂[−], and 217 for CH₃COO[−]. Moreover, alkylammonium PILs have definitely larger heat storage densities than BMIImBF₄. All values are much higher than the minimum storage density (1.9 $MJ \cdot m^{-3}$) specified by the American National Renewable Energy Laboratory,³⁸ indicating that these PILs could be potentially used as excellent heat-transfer fluids.

3.4. Effect of Water on the Specific Gravity, Conductivity, and Viscosity of PILs.

In Figure 5, we present the density of aqueous solutions of DIPEF versus concentration expressed in weight percentage of water. Specific gravity values increase when the proportion of water increases in the mixture until a maximum ranging at 20–30% of water. This comportment is different from what has been reported for aqueous solutions of 1-butyl-3-methyl imidazolium tetrafluoroborate (BMIImBF₄)^{20,21} for which specific gravity values monotonically decrease with the amount of water in the mixture.

Density measurements are fitted to a polynomial expression of the form

$$\rho = \sum_{k=0}^m A_k w^k \quad (3)$$

where A_k are the fitting parameters and w represents the mass percentage of the water in the aqueous mixture. The maximal value of the exponent k was chosen to obtain a regression factor, $R^2 > 0.999$. The obtained A_k parameters are summarized in Table 6 for PILs.

On the graph reported in Figure 6a, three different zones can be clearly defined: (I) below 60% of water, i.e., water in the PILs zone, a continuous increase in conductivity occurs as the viscosity decreases faster than the decrease in ionic species concentration occurring by dilution; (II) between 60% and 75% in water, a transition zone is observed for which the decreasing viscosity is compensated by the dilution effect; (III) for more than 75% in water, the dilution effect is predominated and the ionic conductivity decreases sharply to almost zero.

Figure 6b shows that the Walden product is not constant. This result is explained by the fact why the increasing of ionic conductivity is not only due to the decreasing of viscosity with the water that is added. Indeed, in the PILs–water mixture, the aggregates must be formed, and so $\Delta\eta$ varies with the composition mixture.[>]

4. Conclusion

The protic subclass of PILs is enormously broad as there are many ways of combining an anion and protic cation. These are proton-transfer salts chosen for their high melting points. A potentially important aspect of this study concerns the demonstrated general existence of high-temperature-stable, proton-rich, ionic liquids. The temperature dependence of ionic conductivity and viscosity for these ionic liquids in the temperature range of 25–120 °C obeys the VTF law. We have also compared the ionicity of ionic liquids with Walden's rule, which relates the equivalent conductance with the dynamic viscosity. Then, we have explored to them "fragility" while basing on the theory developed by Angell. Finally, the thermal properties of the ionic liquids presented here indicate that they are suited for use as heat-transfer fluids. The values of the ionic conductivity of PILs–water mixtures are 8 times higher than the value that presents the pure PILs. Despite their high proton contents, these liquids are not as aggressive as might be expected; their physical and thermal properties, cost, and availability will be important future issues. Finally, we will note that these members of the ILs family, those produced by transfer of a proton from one molecular species to another, can serve as excellent proton-transfer media for fuel cells of a novel type.³⁹

References and Notes

- (1) Wilkes, J. S. *Green Chem.* **2002**, *4*, 73.
- (2) Welton, T. *Chem. Rev.* **1999**, *99*, 2071.
- (3) Wasserscheid, P.; Keim, W. *Angew. Chem.* **2000**, *112*, 3926.
- (4) Carpio, R. A.; King, L. A.; Lindstrom, R. E.; Nardi, J. C.; Hussey, C. L. *J. Electrochem. Soc.* **1979**, *126*, 1644.
- (5) Enders, F. *Phys. Chem.* **2004**, *218*, 255.
- (6) Jarosik, A.; Krajewski, S. R.; Lanndowski, A.; Radzinski, P. *J. Mol. Liq.* **2006**, *123*, 43.
- (7) Pappenfus, T. M.; Henderson, W. A.; Owens, B. B.; Mann, K. R.; Smyrl, W. H. *J. Electrochem. Soc.* **2004**, *151*, 209.
- (8) Lewandowski, A.; Swiderska, A. *Solid State Ionics* **2004**, *169*, 21.
- (9) Noda, A.; Hayamizu, K.; Watanabe, M. *J. Phys. Chem. B* **2001**, *105*, 4603.
- (10) MacFarlane, D. R.; Meakin, P.; Sun, J.; Amini, N.; Forsyth, M. *J. Phys. Chem. B* **1999**, *103*, 4164.
- (11) Tokuda, H.; Tsuzuki, S.; Susan, M. A. B. H.; Hayamizu, K.; Watanabe, M. *J. Phys. Chem. B* **2006**, *110*, 19593.
- (12) Zhou, Z.-B.; Hajime, M.; Tatsumi, K. *Chem. Lett.* **2004**, *33*, 886.
- (13) Xu, W.; Wang, L.-M.; Nieman, R. A.; Angell, C. A. *J. Phys. Chem. B* **2003**, *107*, 11749.
- (14) Xu, W.; Cooper, E. I.; Angell, C. A. *J. Phys. Chem. B* **2003**, *107*, 6170.
- (15) Forsyth, S. A.; MacFarlane, D. R. *J. Mater. Chem.* **2003**, *13*, 2451.
- (16) Noda, A.; Susan, M. A. B. H.; Kudo, K.; Mitsushima, S.; Hayamizu, K.; Watanabe, M. *J. Phys. Chem. B* **2003**, *107*, 4024.
- (17) Susan, M. A. B. H.; Noda, A.; Mitsushima, S.; Watanabe, M. *Chem. Commun.* **2003**, 938.
- (18) Matsuoka, H.; Nakamoto, H.; Susan, M. A. B. H.; Watanabe, M. *Electrochim. Acta* **2005**, *50*, 4015.
- (19) Yamada, M.; Honma, I. *Electrochim. Acta* **2003**, *48*, 2411.
- (20) Yoshizawa, M.; Ohno, H. *Chem. Commun.* **2004**, 1828.
- (21) Anouti, M.; Caillon-Caravanier, M.; Le Floch, C.; Lemordant, D. *J. Phys. Chem. B* **2008**, *112*, 9406.
- (22) Walden, P. Z. *Phys. Chem.* **1906**, *55*, 207, 246.
- (23) Bockris, J. O. M.; Reddy, A. K. N. *Modern Electrochemistry*, 2nd ed.; Plenum Press: New York, 1998.
- (24) Matsumoto, H.; Yanagida, M.; Tanimoto, K.; Nomura, M.; Kitagawa, Y.; Miyazaki, Y. *Chem. Lett.* **2000**, *29*, 922.
- (25) Forsyth, S.; Golding, J.; MacFarlane, D. R.; Forsyth, M. *Electrochim. Acta* **2001**, *46*, 1753.
- (26) Matsumoto, H.; Matsuda, T.; Hagiwara, R.; Ito, Y.; Miyazaki, Y. *Chem. Lett.* **2001**, *30*, 26.
- (27) Tsuda, T.; Nohira, T.; Nakamori, Y.; Matsumoto, K.; Higawara, R.; Ito, Y. *Solid State Ionics* **2002**, *149*, 295.
- (28) Angell, C. A. *Science* **1995**, *267*, 1924.
- (29) Ediger, M. D.; Angell, C. A.; Nagel, S. R. *J. Phys. Chem.* **1996**, *100*, 13200.
- (30) Angell, C. A.; MacFarlane, D. R.; Oguni, M. *Ann. N.Y. Acad. Sci.* **1986**, *484*, 241.
- (31) Donth, E. *J. Non-Cryst. Solids* **1982**, *53*, 325.
- (32) Hodge, I. M. *J. Non-Cryst. Solids* **1996**, *202*, 164.
- (33) Böhmer, R.; Angell, C. A. *Phys. Rev. B* **1992**, *45*, 10091.
- (34) Kokshenev, V. B.; Borges, P. D.; Sullivan, N. S. *J. Chem. Phys.* **2005**, *122*, 114510.
- (35) Richert, R.; Angell, C. A. *J. Chem. Phys.* **1998**, *108*, 9016.
- (36) Angell, C. A. *J. Phys. Chem. Solids* **1988**, *49*, 863.
- (37) Belieres, J.-P.; Angell, C. A. *J. Phys. Chem. B* **2007**, *111*, 4926.
- (38) Van Valkenburg, M. E.; Vaughn, R. L.; Williams, M.; Wilkes, J. S. *Thermochim. Acta* **2005**, *425*, 181.
- (39) Martinez, L. M.; Angell, C. A. *Nature* **2001**, *410*, 663.

JP803489N